Environmental Pollution 236 (2018) 926–936

Contents lists available at ScienceDirect

Environmental Pollution

journal homepage: www.elsevier.com/locate/envpol

Mitochondrial dysfunction, perturbations of mitochondrial dynamics and biogenesis involved in endothelial injury induced by silica nanoparticles☆

Caixia Guo [a, b], Ji Wang [b, c], Li Jing [b, c], Ru Ma [a, b], Xiaoying Liu [b, c], Lifang Gao [b], Lige Cao [b, c], Junchao Duan [b, c], Xianqing Zhou [b, c], Yanbo Li [b, c, *], Zhiwei Sun [b, c]

[a] Department of Occupational Health and Environmental Health, School of Public Health, Capital Medical University, Beijing 100069, China
[b] Beijing Key Laboratory of Environmental Toxicology, Capital Medical University, Beijing 100069, China
[c] Department of Toxicology and Sanitary Chemistry, School of Public Health, Capital Medical University, Beijing 100069, China

ARTICLE INFO

Article history:
Received 19 May 2017
Received in revised form
9 October 2017
Accepted 14 October 2017
Available online 1 November 2017

Keywords:
Silica nanoparticle
Endothelium
Mitochondrial dynamics
Biogenesis
Oxidative stress

ABSTRACT

As silica nanoparticles (SiNPs) pervade the global economy, however, the followed emissions during the manufacturing, use, and disposal stages inevitably bring an environmental release, potentially result in harmful impacts. Endothelial dysfunction precedes cardiovascular disease, and is often accompanied by mitochondrial impairment and dysfunction. We had reported endothelial dysfunction induced by SiNPs, however, the related mechanisms by which SiNPs interact with mitochondria are not well understood. In the present study, we examined SiNPs-induced mitochondrial dysfunction, and further demonstrated their adverse effects on mitochondrial dynamics and biogenesis in endothelial cells (HUVECs). Consequently, SiNPs entered mitochondria, caused mitochondrial swelling, cristae disruption and even disappearance. Further analyses revealed SiNPs increased the intracellular level of mitochondrial reactive oxygen species, eventually resulting in the collapse of mitochondrial membrane potential, impairments in ATP synthesis, cellular respiration and the activities of three ATP-dependent enzymes (including Na^+/K^+-ATPase, Ca^{2+}-ATPase and Ca^{2+}/Mg^{2+}-ATPase), as well as an elevated intracellular calcium level. Furthermore, mitochondria in SiNPs-treated HUVECs displayed a fission phenotype. Accordingly, dysregulation of the key gene expressions (FIS1, DRP1, OPA1, Mfn1 and Mfn2) involved in fission/fusion event further certified the SiNPs-induced perturbation of mitochondrial dynamics. Meanwhile, SiNPs-treated HUVECs displayed declined levels of mitochondrial DNA copy number, PGC-1α, NRF1 and also TFAM, indicating an inhibition of mitochondrial biogenesis triggered by SiNPs via PGC-1α-NRF1-TFAM signaling. Overall, SiNPs triggered endothelial toxicity through mitochondria as target, including the induction of mitochondrial dysfunction, as well as the perturbations of their dynamics and biogenesis.

1. Introduction

Silica nanoparticles (SiNPs) are among the nanomaterials most frequently utilized in products on the global market. It is widely used as additives for food, cosmetics, drugs, varnishes and printer toners. It was estimated that a consumer intake of nanoscale silica from food was about 1.8 mg·kg bw^{-1}·d^{-1} (Dekkers et al., 2011). Furthermore, these NPs are being applied in biomedical and biotechnological fields, e.g., drug or DNA delivery, enzyme immobilization, bioimaging, diagnosis, and even cancer therapy. Consequently, the anticipated increases in the production and application of SiNPs in the industrial, commercial, and biomedical fields inevitably result in an increase in their environmental presence (Keller et al., 2013). Currently, SiNPs is on the lists for toxicity evaluation by the Organization for Economic Cooperation and Development (OECD) and the National Institute of Environmental Health Sciences (NIEHS). Reportedly, ultrafine particles (UFP) in which silica is inorganic component are widely spread in the atmosphere through sandstorm, construction and combustion processes (Asweto et al., 2017). Epidemiological evidences have confirmed the correlation

☆ This paper has been recommended for acceptance by Baoshan Xing.

* Corresponding author. Department of Toxicology and Sanitary Chemistry, School of Public Health, Capital Medical University, No.10 Xitoutiao, You An Men, Beijing 100069, China.
E-mail address: ybli@ccmu.edu.cn (Y. Li).

https://doi.org/10.1016/j.envpol.2017.10.060
0269-7491/

between the nano-scale UFP and cardiovascular disease (Aguilera et al., 2016). Furthermore, the increasing evidence points to the specific adverse effects of SiNPs on cardiovascular events (Yu et al., 2016). The endothelium is critical to the maintenance of vascular homeostasis. Endothelial dysfunction precedes cardiovascular disease (Rocha et al., 2010). Endothelial injury is an important mechanistic event by which the inhaled particles have effects on the prevalence of cardiovascular disease (Mills et al., 2009). It is well-documented that SiNPs exposure was associated with endothelial dysfunction (Duan et al., 2014b; Guo et al., 2015; Guo et al., 2016), impaired vascular homeostasis (Corbalan et al., 2011; Duan et al., 2014a; Nemmar et al., 2014), and consequently cardiovascular diseases. However, the underlying mechanisms by which SiNPs interact with, and affect the functions of cellular components in endothelium, are still unclear and not well understood.

The mitochondrion serves essential roles in cell metabolism, ROS generation, redox regulation, calcium (Ca^{2+}) homeostasis, cell proliferation, cell cycle progression and cell death, as well as cellular energy transduction and adenosine triphosphate (ATP) production. A series of studies have shown mitochondria as the potentially relevant target organelles for nanoparticles (NPs) toxicity (Fujioka et al., 2014). We ever observed SiNPs deposited inside mitochondria, caused mitochondrial damage, collapse of mitochondrial membrane potential ($\Delta\Psi m$), resulting in the mitochondrial-mediated apoptosis in HepG2 cells (Sun et al., 2011). Similarly, SiNPs did impairments to mitochondrial dehydrogenase activity, $\Delta\Psi m$ and respiratory chain complexes activities in hepatocytes (Xue et al., 2014). Endothelial mitochondria are essential to the vascular pathophysiology, considering as “frontline against vascular disease” (Davidson and Duchen, 2007), while its dysfunction would inevitably result in a collapse of endothelial homeostasis. However, how SiNPs interact with mitochondria (e.g. mitochondrial dynamics, biogenesis) and thus affect endothelial function still remains unknown.

Mitochondria continually undergo fusion and fission - two apparently opposite and highly regulated processes. Mitochondrial fusion and fission, termed as mitochondrial dynamics, is crucial to the maintenance of mitochondrial shape, size, number, and even function. In brief, mitochondrial fission is regulated by dynamin-related protein-1 (DRP1) and Fission-1 (FIS1), while fusion by mitofusins (Mfn1, Mfn2) and optic atrophy 1 (OPA1). Furthermore, mitochondrial biogenesis in cooperation with mitophagy determines mitochondrial content, structure, and function, and participates in cell metabolism, oxidative stress, and signal transduction. Damage to mitochondrial dynamics and biogenesis is vital in cardiovascular disease (Dorn et al., 2015). In this study, the adverse effects of SiNPs on endothelial mitochondrion were investigated, including its structure, function, dynamics and also biogenesis. Additionally, the master regulator of mitochondrial biogenesis peroxisome proliferator-activated receptor gamma coactivator-1α (PGC-1α), and its downstream targets - nuclear respiratory factor 1 (NRF1) and mitochondrial transcription factor A (TFAM), were determined. To our best knowledge, we report for the first time that SiNPs induce perturbations of mitochondrial dynamic and biogenesis via the PGC-1α-NRF1-TFAM signaling, resulting in mitochondrial dysfunction in endothelial cells. Our research reveals the details of those previously observed effects referred to SiNPs, which is vital for the understanding of NP-related potential human health issues.

2. Materials and methods

2.1. Materials

The preparation and characterization of SiNPs have already been described in our previous study (Guo et al., 2015). Endothelial cell line, HUVECs (human umbilical vein endothelial cells) was purchased from the Cell Resource Center, Shanghai Institutes for Biological Sciences, China. Both MTT and JC-1, a fluorescent probe for $\Delta\Psi m$ determination, were obtained from Sigma-Aldrich, USA. Fetal bovine serum (FBS), Dulbecco's modified Eagle's medium (DMEM), and MitoSOX™ were acquired from Thermo Fisher Sientific, USA. MitoTracker Green and Fluo-3 AM were purchased from Beyotime, China. The Na^+/K^+-ATPase, Ca^{2+}-ATPase and Ca^{2+}/Mg^{2+}-ATPase activity assay kits were supplied by Nanjing Jianchen Bioengineering Institute, China.

2.2. Cell culture and treatment

HUVECs were cultured in DMEM supplemented with 10% FBS at 37 °C in a 5% CO_2 humidified incubator. Cells were incubated up to about 24 h and grown to about 80% confluence before experiments. SiNPs were dispersed in deionized water, and diluted to appropriate concentrations by DMEM culture medium. After SiNPs treatment, cells were collected for a series of analyses according to the experiment schedule.

2.3. SiNP uptake and cellular ultrastructure observation

After 50 $\mu g \cdot mL^{-1}$ SiNPs treatment for 24 h, HUVECs cells were collected for the observation of SiNPs uptake and cellular ultrastructure by using TEM as previously described (Guo et al., 2016).

2.4. Mitochondrial activity analysis

The reduction of MTT to formazan was dependent on the activity of mitochondrial succinode hydrogenase. Thus mitochondrial activity of HUVECs was analyzed using the MTT assay (Souza et al., 2014; Tvrda et al., 2016). Briefly, 1×10^4 HUVEC cells were placed in each of 96 wells. On the next day, after twice rinse by phosphate buffered saline (PBS), the cells were incubated with SiNPs (dose: 0, 12.5, 25, 50 and 100 $\mu g \cdot mL^{-1}$ respectively) for 6, 12, 24, 48 or 72 h at 37 °C. At last, the absorbance (A_{490}) was measured by a microplate reader (SpectraMax M5; Molecular Devices, USA).

2.5. Mitochondrial ROS (mtROS) measurement

The mtROS production was measured using MitoSOX™, a mitochondrial superoxide indicator. MitoTracker Green, a selective mitochondrial fluorescent probe that is not affected by $\Delta\Psi m$, was used for the specific staining of endothelial mitochondria. HUVECs were treated with 50 $\mu g \cdot mL^{-1}$ SiNPs for 24 h, after that, cells were co-stained with 5 μM MitoSOX™ and 100 nM MitoTracker Green in serum free culture medium at 37 °C for 30 min in the darkness. The cells were extensive washed with phosphate buffered saline (PBS) and then observed under a laser scanning confocal microscope, LSCM (LSM 710; Zeiss, Germany). Moreover, the MitoSox™ fluorescence intensity was also determined using a flow cytometer (Becton-Dickinson, USA).

2.6. $\Delta\Psi m$ assay

JC-1 probe can selectively enter into mitochondria, and its red/green ratio is frequently used to reflect the change of $\Delta\Psi m$. After SiNPs treatment for 24 h, cells were washed with PBS for three times, and then incubated with JC-1 working solution, 10 $mg \cdot L^{-1}$ for 20 min. At last, the cells were observed under LSCM. Meanwhile, the red/green ratio was analyzed by Leica QWin image analysis software (Leica Microsystems, Wetzlar, Germany). At least 20 fields were picked in each group for the measurement of mean values of

red and green fluorescence intensities, and then the mean value of red/green ratio was calculated.

2.7. Cellular ATP production assay

The cellular ATP production was measured by using a Luciferase-Based Luminescence Assay Kit (Beyotime, China). ATP content was normalized to protein concentration, and expressed as μmol/g protein.

2.8. Intracellular calcium level detection

After 50 $\mu g \cdot mL^{-1}$ SiNPs treatment for 24 h, cells were washed with PBS for three times, and then incubated with Ca^{2+} indicator, Fluo-3 AM (5 $\mu mol\,L^{-1}$) for 20 min. Ultimately, the cells were imaged under LSCM.

2.9. Mitochondrial morphology imaging

After 50 $\mu g \cdot mL^{-1}$ SiNPs exposure for 24 h, cells were incubated with 100 nM MitoTracker Green in darkness for 30 min, and then washed extensively and imaged using LSCM.

2.10. Mitochondrial DNA (mtDNA) copy number determination

Real-time PCR was used for the relative quantification of mtDNA copy number. The total intracellular DNA was extracted using QIAampDNA mini kit (QIAGEN, USA) according to the manufacturer's instruction. 12S rRNA and β-actin were used as the marker for mtDNA and nuclear DNA (nDNA, as internal control), respectively. See supplementary file for the primer sequence.

2.11. Quantitative real-time RT-PCR analysis

The relative amounts of the subunits of mitochondrial electron transfer complex (METC), including MT-CYB, MT-ATP6, MT-CO1 and MT-ND1, and also mitochondrial dynamics related factors, such as DNM1L (also known as DRP1), FIS1, OPA1, MFN1 and MFN2, were quantified by real-time RT-PCR. β-actin was set as an internal standard. The primer sets are listed in supplementary file.

2.12. Na^+/K^+-ATPase, Ca^{2+}-ATPase, and Ca^{2+}/Mg^{2+}-ATPase activities determination

The activities of Na^+/K^+-ATPase, Ca^{2+}-ATPase and Ca^{2+}/Mg^{2+}-ATPase were measured by using a commercial kit according to the manufacturer's protocols.

2.13. Western blot analysis

The protein levels of FIS1, DRP1, OPA1, Mfn1, Mfn2, PGC-1α, TFAM, and also NRF1 in HUVECs were determined by Western blot analysis. GAPDH was also detected as the internal control. The primary antibodies were all acquired from Cell Signaling Technology, USA. The photodensitometric analysis of the protein band was done using Image Lab™ Software (Bio-Rad, USA).

2.14. Statistical analysis

Data were presented as means ± SD. The significant analysis of mRNA and protein expressions of factors involved in the mitochondrial fusion/fission was determined by Student's t-test, whereas that for other data was analyzed using one-way analysis of variance (ANOVA). All comparisons were two-tailed and statistical significance was set at $p < 0.05$.

3. Results

3.1. Characterization of SiNPs

Under TEM observation, SiNPs manifested a spherical or near-spherical shape and relatively favorable dispersibility (Fig. 1). The SiNPs was fully characterized in our previous study (Guo et al., 2015): its average diameter was approximately 57.66 ± 7.30 nm. Furthermore, its hydrodynamic sizes and Zeta potentials in either DMEM or distilled water displayed good monodispersity. Additionally, it was endotoxin-free with purity more than 99.9%. These results demonstrated SiNPs possessed uniform shape, favorable stability and dispersibility in the culture medium.

3.2. Cellular uptake of SiNPs

As shown in Fig. 2, SiNPs were taken up by HUVECs, and dispersed in cytoplasm either free or as membrane-bound aggregates, while not observed in nucleus.

3.3. Morphological change in mitochondria induced by SiNPs

To investigate the damage caused by SiNPs in HUVECs, especially that in mitochondria, the further ultrastructural analysis revealed that SiNPs were found to deposit in mitochondria, and the SiNPs-treated cells manifested significant ultrastructure changes in mitochondria, including cristae rupture, disappearance, and mitochondrial swelling, whereas the control cells with normal intact mitochondria (Fig. 3).

3.4. Mitochondrial activity decline induced by SiNPs

The results acquired from MTT assay showed that mitochondrial activity of HUVECs cells decreased in a dose- and time-dependent manner following SiNPs exposure (Fig. 4). The IC_{50} of SiNPs for HUVECs was 48.99 $\mu g \cdot mL^{-1}$ after 24 h exposure.

3.5. mtROS generation triggered by SiNPs

The production of mtROS increased after SiNPs exposure, indicating SiNPs triggered mitochondria for ROS generation, and further led to oxidative stress in HUVECs (Fig. 5).

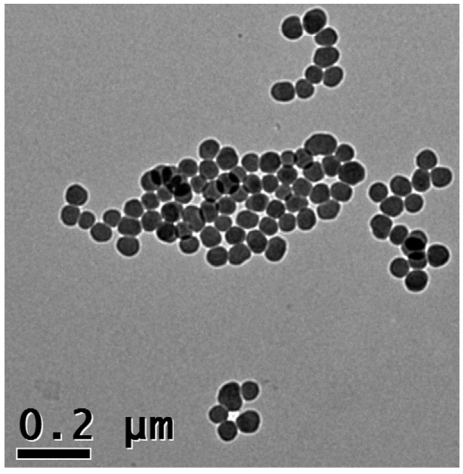

Fig. 1. Representative TEM image of tested SiNPs. All particles were near-spherical in shape, and had good monodispersity. The scale bar, 0.2 μm.

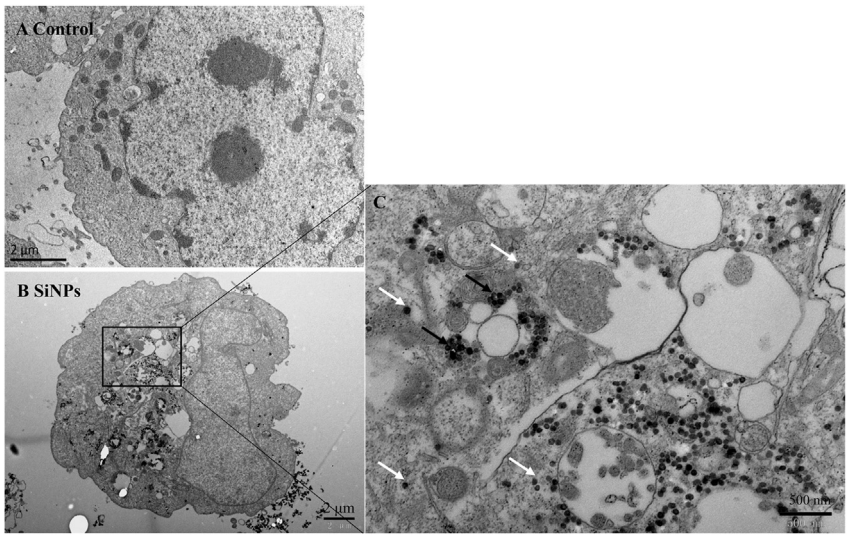

Fig. 2. Typical TEM images showing cellular uptake of the SiNPs in HUVECs. (A) Control group. (B) SiNPs group. HUVECs were treated with 50 μg mL^{-1} SiNPs for 24 h. (C) The magnification of selected area of SiNPs group. The electron-dense SiNPs dispersed in cytoplasm either free (white arrow) or as membrane-bound aggregates (black arrow) can be clearly observed, but no particles in nucleus.

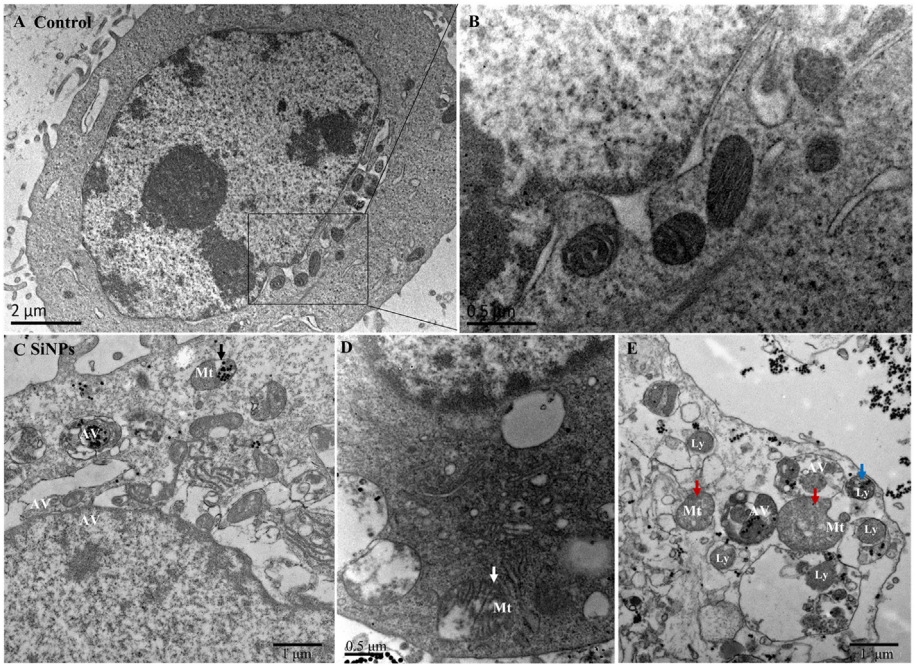

Fig. 3. The ultrastructure alterations in mitochondria induced by SiNPs in HUVECs observed by TEM. (A) Control group. (B) The magnification of selected area of Control group showed evidently intact mitochondria. The mitochondria were round or elongated and the structure of cristae were regular. (C–E) SiNPs group. HUVECs were treated with 50 μg mL^{-1} SiNPs for 24 h. Cytoplasmic cavitation and irregular mitochondria were observed. The SiNPs deposited in mitochondria (Mt, black arrow). The induction of cristae rupturing and disappearance (white arrow), as well as mitochondrial swelling (red arrow) can be clearly observed in SiNPs-treated HUVECs. SiNPs also induced autophagy, characterized by a number of autophagic vacuole (AV) in cytoplasm, which contains the degraded cytoplasmic contents and highly electron-dense SiNPs. Besides mitochondria (Mt), SiNPs also deposited in the lysosomes (Ly, blue arrow), and did impairment to lysosomes. (For interpretation of the references to colour in this figure legend, the reader is referred to the web version of this article.)

3.6. *ΔΨm collapse induced by SiNPs*

Along with the increasing concentrations of SiNPs exposure, the HUVECs manifested the gradually enhanced cytoplasmic diffusion of green monomer fluorescence, and whereas the weakened red aggregate fluorescence (Fig. 6A). Indeed, the further quantitative analysis of red/green ratio revealed a dose-dependent decline of ΔΨm induced by SiNPs (Fig. 6B).

3.7. *Mitochondrial dysfunction induced by SiNPs*

The ATP production in HUVECs was significantly suppressed by SiNPs (Fig. 7A). MT-ND1, MT-CYB, MT-CO1, and MT-ATP6 in turn are the subunits of METC complex I, III, IV and V. Their mRNA expressions were all significantly decreased after SiNPs treatment, revealing an inhibitory effect of SiNPs on electron transfer and cellular respiration (Fig. 7B). Besides, SiNPs caused an obviously

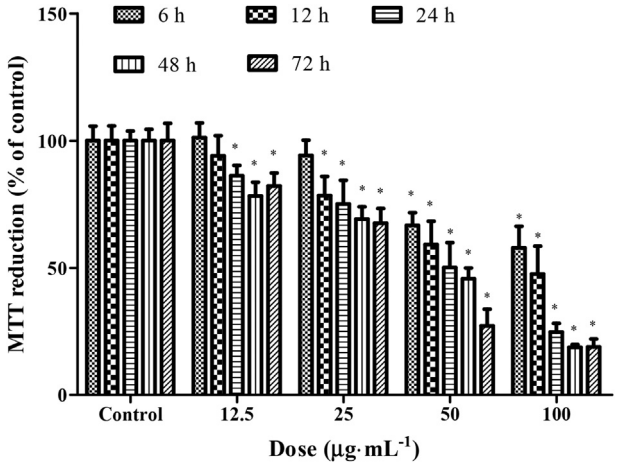

Fig. 4. Dose- and time-dependent decreases of mitochondrial activity in HUVECs induced by SiNPs. Data are expressed as mean ± S.D. of three independent experiments. *$p < 0.05$ vs control.

elevated intracellular Ca^{2+} level (Fig. 7C), and declined activities of Na^{+}/K^{+}-ATPase, Ca^{2+}-ATPase and Ca^{2+}/Mg^{2+}-ATPase (Fig. 7D). All these results indicated SiNPs induced mitochondrial dysfunction in endothelial cells.

3.8. Perturbation of mitochondrial dynamics induced by SiNPs

Firstly, mitochondrial shape was observed using MitoTracker Green staining (Fig. 8A). The control endothelial mitochondrion manifested the typical fiber-like morphology, whereas the SiNPs-treated mitochondrion presented fragmentation, suggesting SiNPs induced a perturbation in mitochondrial dynamics, and shifted mitochondrial morphology toward a fission type. The further relative expressions of mitochondrial fusion/fission markers showed that under the SiNPs exposure, FIS1, DRP1 and Mfn2 were up-regulated, and OPA1 and Mfn1 were down-regulated in either mRNA and/or protein levels (Fig. 8B–D). These results indicated that the abnormal expressions of these key factors involved in mitochondrial fission/fusion event may contribute to the SiNPs-induced imbalance in mitochondrial dynamics, which eventually favors fission.

3.9. Inhibition of mitochondrial biogenesis induced by SiNPs

A decline in mtDNA copy number was found in HUVECs after SiNPs treatment ($p < 0.05$, Fig. 9A). Moreover, the protein levels of PGC-1α, NRF1 and TFAM were significantly decreased in HUVECs after SiNPs treatment ($p < 0.05$, Fig. 9B and C). These data revealed that SiNPs inhibited mitochondrial biogenesis in HUVECs, which might be mediated by PGC-1α-NRF1-TFAM signaling.

4. Discussion

Endothelial mitochondria have a prominent role in signaling cellular responses to environmental cues. The damage to mitochondrion is frequently observed in cardiovascular disease, and probably contributes to the multiple pathophysiological processes

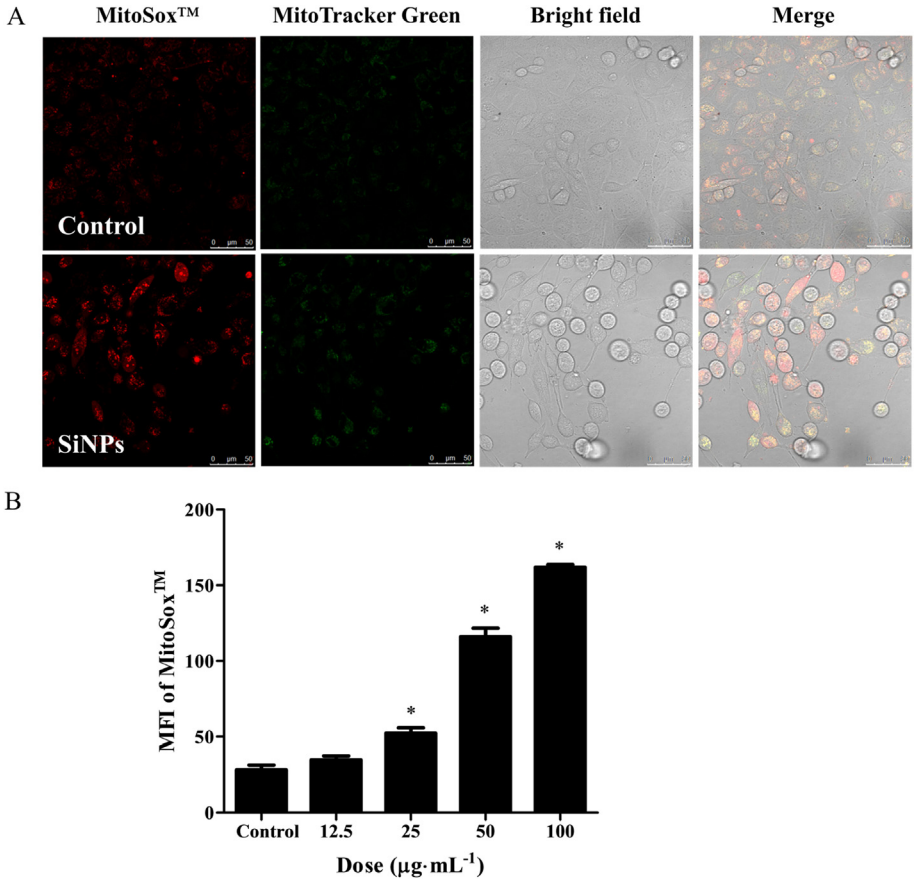

Fig. 5. mtROS generation triggered by SiNPs in HUVECs. (A) The confocal images of HUVECs costained with MitoSOX™ and MitoTracker Green fluorescent probes. (B) Quantification of the MitoSOX™ fluorescence via FCM for the determination of mtROS. Data are expressed as means ± S.D. from three independent experiments. *$p < 0.05$ vs control.

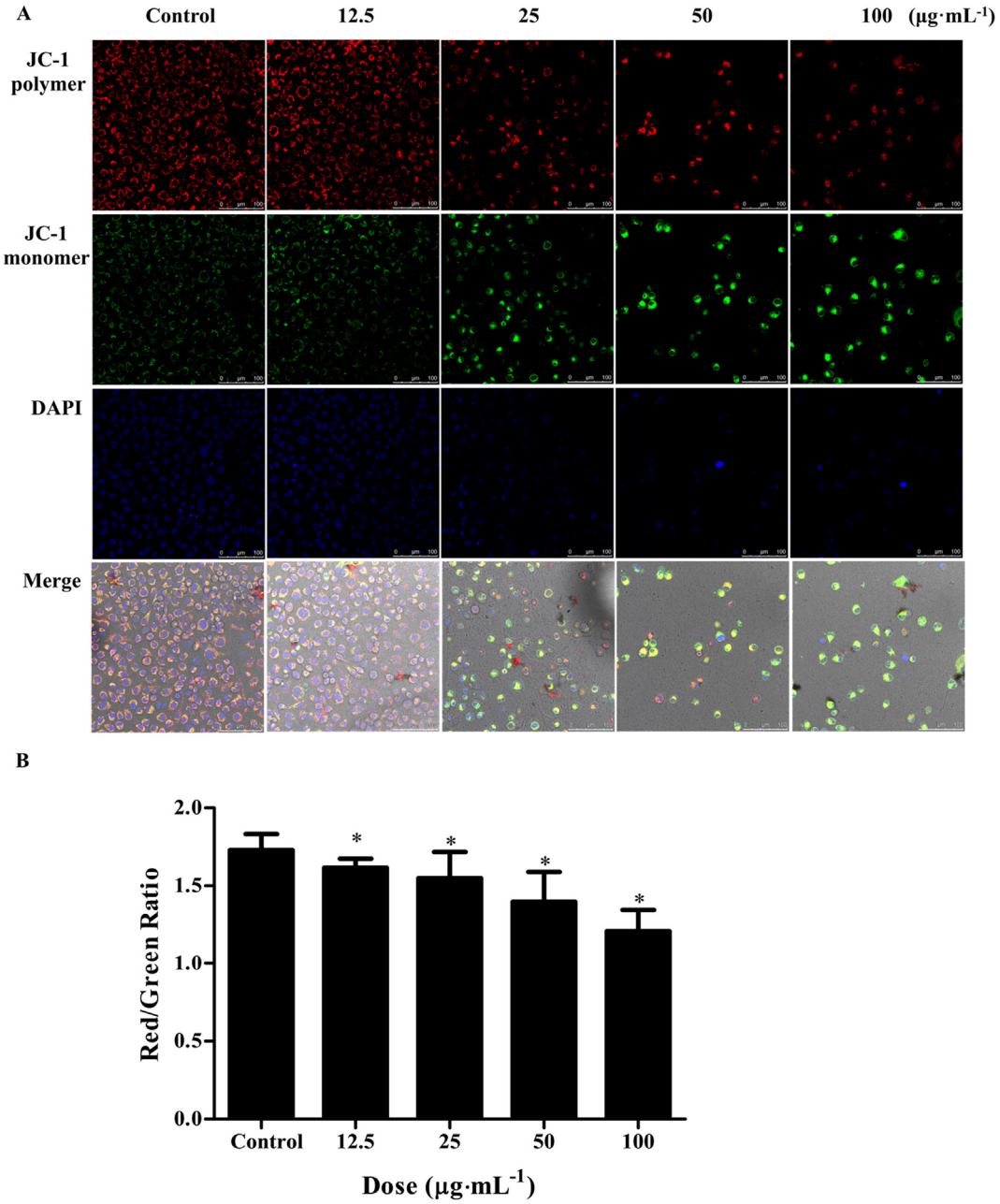

Fig. 6. The ΔΨm decline induced by SiNPs in HUVECs. (A) Confocal images of ΔΨm. (B) The JC-1 Red/Green fluorescence intensity ratio. Data are expressed as means ± S.D. from three independent experiments. $^{*}p < 0.05$ vs control.

(for instance energy imbalance, oxidative injury, endothelial dysfunction) underlying cardiovascular disease (Marzetti et al., 2013; Yu et al., 2012). The induction of endothelial dysfunction by SiNPs has already been confirmed *in vitro* and *in vivo* (Bauer et al., 2011; Du et al., 2013; Guo et al., 2015). Most notably, mitochondria have been suggested as the major target for NPs exposure (Dong et al., 2016; Nguyen et al., 2015; Sun et al., 2011; Wilson et al., 2015). SiNPs could enter and accumulate in mitochondria once these particles enter into cells (Sun et al., 2011), however, their toxicological effects on mitochondrion have not been extensively investigated. Here, we demonstrated the alterations of mitochondrial structure and morphology induced by SiNPs, which was closely connected with oxidative stress, and also perturbations of mitochondrial dynamics and biogenesis. In line with this notion, we also found a substantial inhibition in expressions of molecules involved in the regulation of mitochondrial biogenesis by SiNPs, including PGC-1α, NRF1 and TFAM. All these results suggested that SiNPs perturb mitochondrial dynamics, biogenesis and function in endothelial cells, which was thus likely to contribute to endothelial dysfunction, and consequently vascular diseases.

The cellular uptake and trafficking of NPs is involved in cellular signaling, which plays an important role in NP-induced toxicity. Studies with gold NPs showed that they did not induce significant cytotoxicity, with no evidence of them entering into mitochondria or nucleus (Wang et al., 2011). Endosomes and lysosomes are considered as the two most common compartments for NP localization (Rejman et al., 2016). Some NPs localize in mitochondria (Hackenberg et al., 2011), and even enter into the nucleus (Raoof

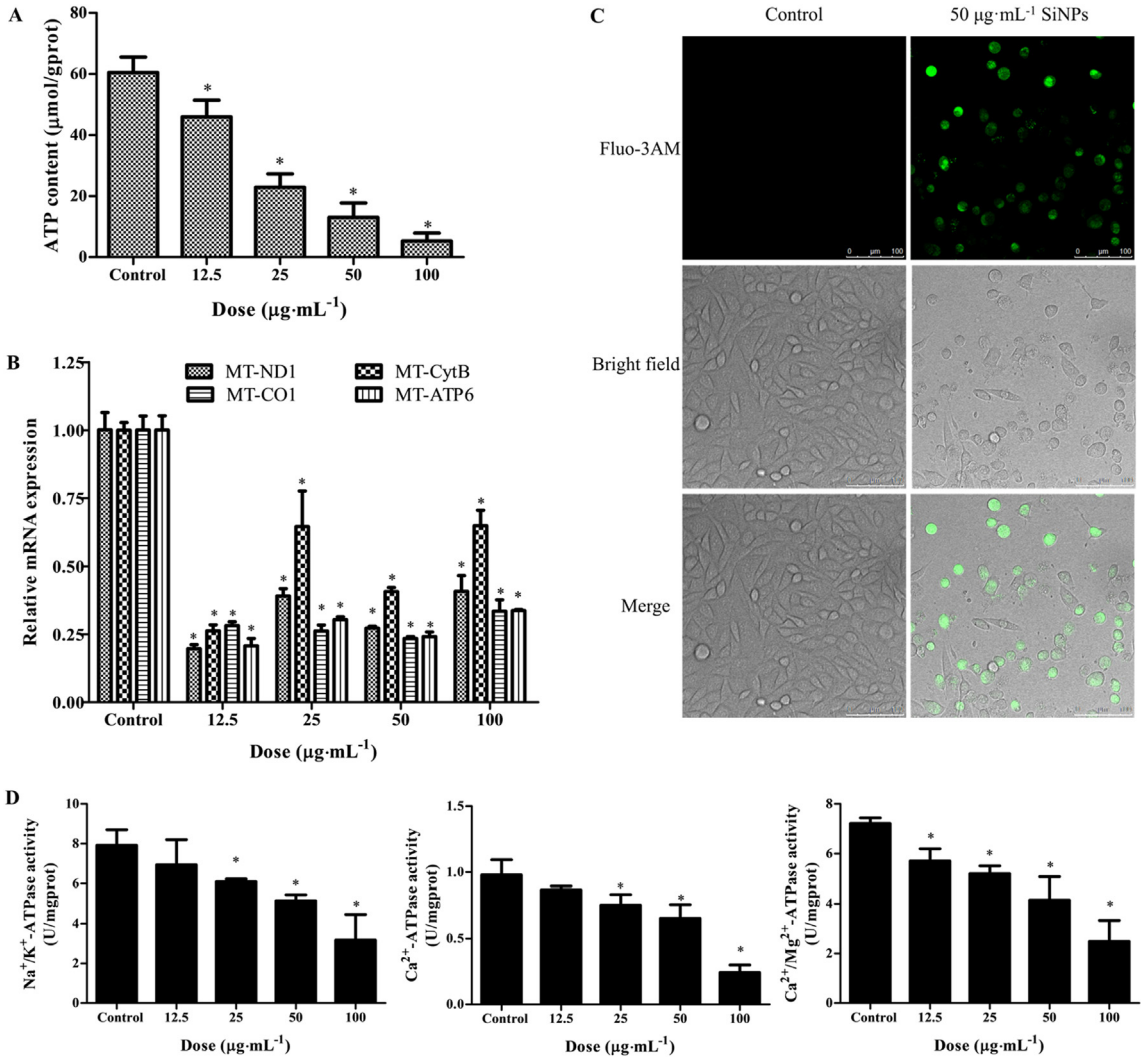

Fig. 7. Mitochondrial dysfunction induced by SiNPs in HUVECs. (A) ATP contents. (B) mRNA expressions of MT-ND1, MT-CYB, MT-CO1, and MT-ATP6, components of METC complex. (C) The representative LSCM image to reveal an elevated intracellular calcium level in HUVECs after 50 μg mL^{-1} SiNPs treatment for 24 h. (D) The activities of Na^+/K^+-ATPase, Ca^{2+}-ATPase and Ca^{2+}/Mg^{2+}-ATPase. Data are expressed as means ± S.D. from three independent experiments. *$p < 0.05$ vs control.

et al., 2012). As indicated in Figs. 2 and 3, we observed an entry of SiNPs into the cytoplasm, especially in lysosome and mitochondria, but not in the nucleus (Figs. 2 and 3). As mitochondria is an important functional compartment of cells playing significant roles in cell metabolism and proliferation, localization of SiNPs in mitochondria may induce severe interference in cellular functions. A decrease in mitochondrial viability is a possible indicator of imminent cell death (Orrenius et al., 2015). As expected, a significant dose- and time-dependent decrease in mitochondrial activity occurred after SiNPs exposure (Fig. 4), also reflecting a loss of endothelial cell viability induced by SiNPs that was consistent with previous findings (Corbalan et al., 2011; Guo et al., 2015; Liu and Sun, 2010). Moreover, SiNPs caused mitochondrial swelling, and cristae disrupture (Fig. 3), which was probably due to the specifically localization of nanoscale particles in mitochondrion (Oberdorster et al., 2005; Xia et al., 2006; Zhu et al., 2006). Similarly, other kinds of nanomaterials, including iron oxide NPs (Zhu et al., 2011), multi-walled nanotubes (Ji et al., 2009), and quantum dots (Nguyen et al., 2015), have also been reported to induce significant alterations in mitochondrial morphology and structure. However, whether the NPs enter in mitochondria via active transport, diffusion or rather indirectly due to mitochondrial membrane damage subsequent to NPs-induced cytotoxic effects via ROS generation, awaits further studies.

Alteration of mitochondrial morphology and structure is closely associated with the impairment of mitochondrial integrity - ΔΨm collapse or loss. The ΔΨm loss in endothelial cells (Fig. 6) might be attributed to the direct interaction between SiNPs and mitochondrion, leading to the physical damage in mitochondria and also regulation of mitochondrial permeability transition pore to depolarize ΔΨm, which in turn, resulting in mitochondrial swelling (Fig. 3F). Besides, mitochondrial membrane depolarization can be caused by the presence of free radicals, high intracellular Ca^{2+} concentration or endoplasmic reticulum stress (Deniaud et al., 2008), which supports our findings that SiNPs promote mtROS generation and enhance intracellular Ca^{2+} level in endothelial cells in this study (Figs. 5 and 7C). The opposite has also been shown in that ΔΨm and intracellular Ca^{2+} level could regulate mtROS generation (Zhang and Gutterman, 2007).

Mitochondria are the major source of ROS production in cells, in turn, are the most adversely affected organelles (Izyumov et al., 2010). Our previous data confirmed ROS induced by SiNPs led to oxidative stress, followed by oxidative injury to endothelial cells (Guo et al., 2015). Exactly, our data manifested a dose-dependent

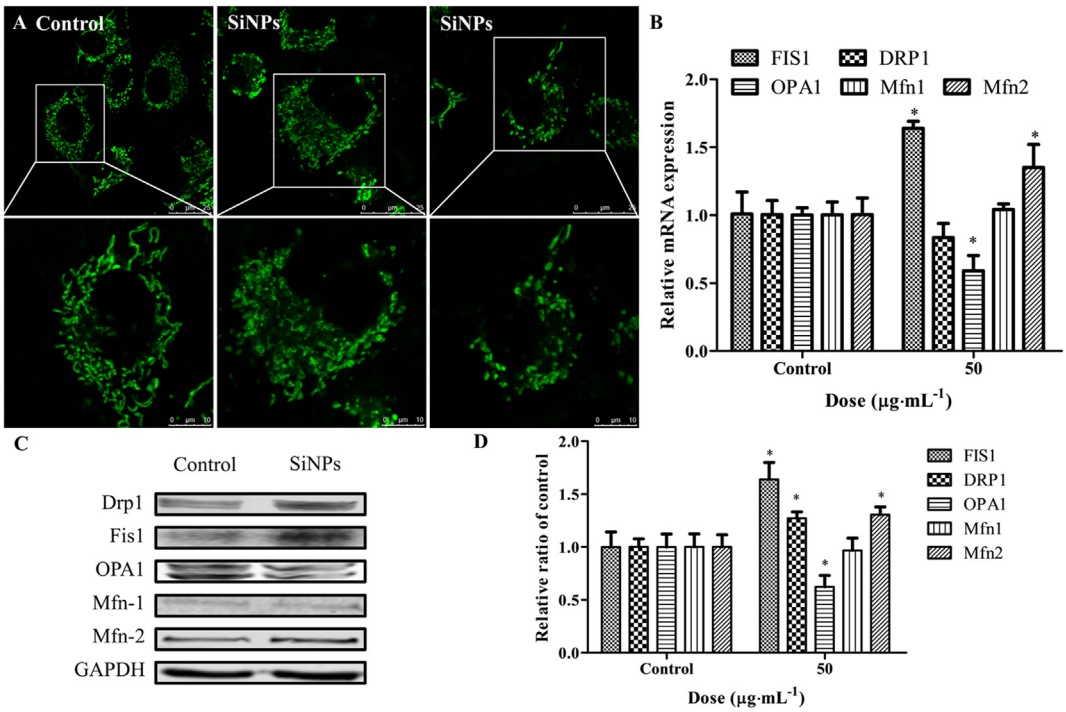

Fig. 8. Perturbation of mitochondrial dynamics induced by SiNPs in HUVECs. The HUVECs were treated with 50 μg mL^{-1} SiNPs for 24 h. (A) Mitochondrial morphology observed under LSCM with MitoTracker Green staining. Relative expressions of mitochondrial fusion/fission markers in both mRNA (B) and protein (C) levels, and the relative densitometric analysis (D) of the protein bands were performed and presented. Data are expressed as the means ± S.D. from three independent experiments. *$p < 0.05$ vs control.

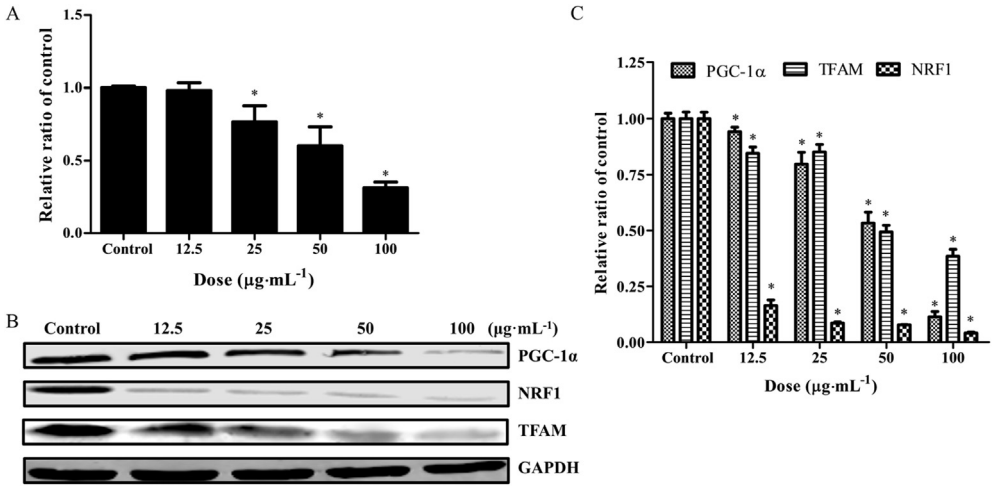

Fig. 9. Inhibition of mitochondrial biogenesis induced by SiNPs in HUVECs via PGC-1α-NRF1-TFAM signaling pathway. (A) mtDNA copy number. (B) Regulation of PGC-1α-NRF1-TFAM signaling pathway. All blots shown are representative of three independent experiments. (C) Relative densitometric analysis of the protein bands. Data are expressed as the mean ± S.D. from three independent experiments. *$p < 0.05$ vs control.

increase of mtROS content after SiNPs treatment (Fig. 5). Excessive ROS will induce modifications to mitochondrial components, including mtDNA, proteins, and lipids, which cause mitochondrial dysfunction, exacerbate ROS production, and eventually set up a vicious cycle that contributes to the pathogenesis of cardiovascular disease (Hill et al., 2012). Within mitochondria, the electron transport chain is the primary site of ROS production. Recently, He et al. reported that METC was identified as a novel target for NPs-mediated cytotoxicity (He et al., 2016). Complexes I and III are considered as the principal sites for the formation of superoxide (O^{2-}). In spite of no measurement of METC activity, the inhibiting mitochondrial complex III subunit will block electron transport to cytochrome *c* leading to enhanced O^{2-} production. Moreover, it is proposed that the inhibition of complex IV subunit MT-CO1 may cause inefficient electron transfer and facilitate "electron leak", thus leading to mtROS generation rather than efficient reduction of O_2 to water.

Mitochondrial function can be the downstream target of oxidative stress. ATP production and cellular respiration are important indicators for mitochondrial function. Previous studies have confirmed that SiNPs treatment impaired mitochondrial function in other cell lines, including the inhibition of cellular respiration and

ATP content (Guerrero-Beltran et al., 2017; Xu et al., 2014). Here, we firstly demonstrated that ATP synthesis in endothelial cells was significantly inhibited by SiNPs, which might be attributed to the NPs' suppression on activities of respiratory chain complexes (Baratli et al., 2014; Chen et al., 2014; Li et al., 2011; Xue et al., 2014). In normal condition, the ΔΨm is maintained by METC. Thus we can conclude that SiNPs induce ΔΨm collapse, then affect METC and further ATP synthesis, and eventually result in mitochondrial dysfunction. In addition, mitochondria serve as calcium buffer site and cooperate with endoplasmic reticulum to regulate the intracellular calcium homeostasis (Camello-Almaraz et al., 2006). The NPs-induced mechanical injury of mitochondria (Rodrigo and Standen, 2005), as well as oxidative stress, can lead to disturbance in calcium homeostasis, which has influence on many aspects of mitochondrial function, such as mtROS production, energy metabolism, mitochondrial dynamics and biogenesis (Duchen, 2000). As shown in Fig. 7C, SiNPs induced an elevated intracellular Ca^{2+} level in endothelial cells. An increase in cytosolic Ca^{2+} concentration may induce Ca^{2+} entry across the mitochondrial inner membrane and cause an elevated Ca^{2+} concentration in the mitochondrial matrix. Meanwhile, the up-regulated mtROS by SiNPs will promote an elevated level of $mtCa^{2+}$ by inhibiting the activity of mitochondrial Na^{+}/Ca^{2+} exchanger (Guo et al., 2013). Na^{+}/K^{+}-ATPase, Ca^{2+}-ATPase and Ca^{2+}/Mg^{2+}-ATPase are essential for homeostatic through maintaining the electrochemical gradient in an energy-dependent manner. Na^{+}/K^{+}-ATPase is an integral membrane protein, which extrudes three Na^{+} molecules in exchange for internalization of two K^{+} molecules through coupling ATP hydrolysis. Plasma membrane Ca^{2+}-ATPase and Ca^{2+}/Mg^{2+}-ATPase are also ATP-hydrolyzing enzymes, and regulate intracellular Ca^{2+} levels through the translocation of Ca^{2+} from the cytosol to the extracellular milieu. In our study, activities of Na^{+}/K^{+}-ATPase, Ca^{2+}-ATPase and Ca^{2+}/Mg^{2+}-ATPase were all significantly reduced after SiNPs treatment (Fig. 7D), which could well-explain the reduced ATP content and intracellular Ca^{2+} overload (Fig. 7A and C). Since ATP is their substrate and also activator, the declined activity of the three ATP-dependent enzymes may be attributed to the particle-induced insufficient ATP production. Studies have also confirmed that intracellular Ca^{2+} level had influence on ATP synthesis through regulating Krebs cycle enzymes and oxidative phosphorylation (Raturi and Simmen, 2013; Szabadkai and Duchen, 2008). Ultimately, the functional impairment of mitochondria initiates cell death.

It is now recognized that the mitochondrial dynamics (continuous mitochondria fission/fusion) enable the endothelial cell not only to meet its metabolic requirements, but also to cope with either internal or external stress (Youle and van der Bliek, 2012). The perturbation of fusion-fission equilibrium alters mitochondrial morphology. Exactly, the SiNPs-treated mitochondria manifested an obvious morphological change from normal fiber-like shape into truncated, even fragmented phenotype (Fig. 8A), indicating a disruption of fusion or enhancement of fission in endothelial mitochondria (Giedt et al., 2012). Studies suggest that cardiovascular disease and other pathological states are correlated with increased mitochondrial fission in endothelium (Ong et al., 2015; Shenouda et al., 2011). Abnormal expressions of proteins involved in fusion/fission regulation have been implicated in varied vascular diseases. In line with the shifted mitochondrial morphology toward a fission type (Fig. 8A), the expressions of FIS1 and DRP1 were greatly increased, while that of OPA1 was declined (Fig. 8B–D), indicating the activation of fission process result in mitochondrial fragmentation. The fission/fusion proteins regulate the formation of cristae (Jendrach et al., 2005), and thus their altered expressions may reflect SiNPs-induced cristae damage (Fig. 3). Besides, fission is beneficial to the selective elimination of damaged mtDNA, however, abundant or uninhibited fission results in poor cell growth and enhances susceptibility to apoptotic stimuli (Scaini et al., 2017), which supports the previous reports that SiNPs cause endothelial apoptosis (Duan et al., 2013; Liu and Sun, 2010). For the fission initiation in various cell lines, low ΔΨm and low ATP levels were necessary, and also high mtROS level was important (Giedt et al., 2012). That could be well-explained our findings that the disruption of mitochondrial dynamic in endothelial cells was closely associated with oxidative stress and further mitochondrial dysfunction by SiNPs exposure.

Besides the perturbation in mitochondrial dynamics, here, SiNPs also caused a decline of mtDNA copy number in endothelial cells. Besides nDNA, mtDNA is highly susceptible to oxidative stress. mtDNA damage has been proposed to be an initiating event in atherogenesis (Ballinger et al., 2002), and closely correlated with the extent of atherosclerosis (Puddu et al., 2005). The DNA damage capacity of SiNPs has been well-documented (Maser et al., 2015). We did observe a significant DNA damage response on endothelial cells after SiNPs exposure (Duan et al., 2013), and also confirmed a decline of mitochondria mass by SiNPs in hepatocytes (Wang et al., 2013). Additionally, other types of NPs-induced disrupture on mtDNA, mitochondrial mass had ever reported (Jaeger et al., 2012; Kang et al., 2011; Lerner et al., 2016). These results suggested that the suppressive effects on mitochondrial biogenesis might be one of the toxic mechanisms among the endothelial dysfunction and consequently cardiovascular diseases induced by NPs exposure. In particular, mitochondrial generation of excess ROS could contribute to the reductions in mitochondrial biogenesis and ultimately mitochondrial dysfunction (Ren et al., 2010). PGC-1α, a master regulator for the mitochondrial biogenesis, has been considered as a potential therapeutic target for mitochondrial diseases (Wenz, 2009). Inhibition of PGC-1α in HUVECs is related to the down-regulation in ATP synthesis and mtDNA copy number (Zuo et al., 2013). The further mechanism exploration revealed that the suppression of mitochondrial biogenesis induced by SiNPs may be mediated by the inhibition of PGC-1α-NRF1-TFAM signaling pathway (Fig. 9). All in all, the alterations in mitochondrial dynamics and biogenesis enable the endothelial cell to remove the damaged mitochondrial components and maintain normal mitochondrial/cellular function in the early stages of disease. Nevertheless, the prolonged perturbations or impairments on these quality-control mechanisms will definitely cause the retention of dysfunctional mitochondria, leading to endothelial dysfunction, and ultimately cardiovascular diseases.

5. Conclusions

In summary, the present study has revealed mitochondrion as the potential intracellular target of SiNPs. Endothelial mitochondrial dysfunction was induced by SiNPs. Moreover, the disturbance of mitochondrial dynamics was certified in SiNPs-treated endothelial cells, as well as the impaired mitochondrial biogenesis probably mediated by inhibiting the PGC-1α-NRF1-TFAM signaling. These impairments in dynamics and biogenesis would lead to mitochondrial dysfunction, oxidative stress, and ultimately cardiovascular disease. To our knowledge, this is the first time to reveal the adverse effects of SiNPs on mitochondrial dynamics and biogenesis in endothelial cells. Therefore, our findings provide evidence for the safety evaluation of NPs. Moreover, mitochondria-directed toxic evaluation has potential for a more comprehensive understanding of NPs' toxicity and their association with various pathological states.

Acknowledgments

The work was supported by the National Natural Science

Foundation of China (81102095, 81230065), Beijing Natural Science Foundation Program (7162021).

Appendix A. Supplementary data

Supplementary data related to this article can be found at https://doi.org/10.1016/j.envpol.2017.10.060.

References

Aguilera, I., Dratva, J., Caviezel, S., Burdet, L., de Groot, E., Ducret-Stich, R.E., Eeftens, M., Keidel, D., Meier, R., Perez, L., Rothe, T., Schaffner, E., Schmit-Trucksass, A., Tsai, M.Y., Schindler, C., Kunzli, N., Probst-Hensch, N., 2016. Particulate matter and subclinical atherosclerosis: associations between different particle sizes and sources with carotid intima-media thickness in the SAPALDIA study. Environ. Health Perspect. 124, 1700–1706.

Asweto, C.O., Wu, J., Hu, H., Feng, L., Yang, X., Duan, J., Sun, Z., 2017. Combined effect of silica nanoparticles and Benzo[a]pyrene on cell cycle arrest induction and apoptosis in human umbilical vein endothelial cells. Int. J. Environ. Res. Public Health 14.

Ballinger, S.W., Patterson, C., Knight-Lozano, C.A., Burow, D.L., Conklin, C.A., Hu, Z., Reuf, J., Horaist, C., Lebovitz, R., Hunter, G.C., McIntyre, K., Runge, M.S., 2002. Mitochondrial integrity and function in atherogenesis. Circulation 106, 544–549.

Baratli, Y., Charles, A.L., Wolff, V., Ben Tahar, L., Smiri, L., Bouitbir, J., Zoll, J., Sakly, M., Auger, C., Vogel, T., Abdelmelek, H., Tebourbi, O., Geny, B., 2014. Age modulates Fe3O4 nanoparticles liver toxicity: dose-dependent decrease in mitochondrial respiratory chain complexes activities and coupling in middle-aged as compared to young rats. Biomed. Res. Int. 2014, 474081.

Bauer, A.T., Strozyk, E.A., Gorzelanny, C., Westerhausen, C., Desch, A., Schneider, M.F., Schneider, S.W., 2011. Cytotoxicity of silica nanoparticles through exocytosis of von Willebrand factor and necrotic cell death in primary human endothelial cells. Biomaterials 32, 8385–8393.

Camello-Almaraz, C., Gomez-Pinilla, P.J., Pozo, M.J., Camello, P.J., 2006. Mitochondrial reactive oxygen species and Ca2+ signaling. Am. J. Physiol. Cell. Physiol. 291, C1082–C1088.

Chen, Y., Wang, Z., Xu, M., Wang, X., Liu, R., Liu, Q., Zhang, Z., Xia, T., Zhao, J., Jiang, G., Xu, Y., Liu, S., 2014. Nanosilver incurs an adaptive shunt of energy metabolism mode to glycolysis in tumor and nontumor cells. ACS Nano 8, 5813–5825.

Corbalan, J.J., Medina, C., Jacoby, A., Malinski, T., Radomski, M.W., 2011. Amorphous silica nanoparticles trigger nitric oxide/peroxynitrite imbalance in human endothelial cells: inflammatory and cytotoxic effects. Int. J. Nanomed. 6, 2821–2835.

Davidson, S.M., Duchen, M.R., 2007. Endothelial mitochondria: contributing to vascular function and disease. Circ. Res. 100, 1128–1141.

Dekkers, S., Krystek, P., Peters, R.J., Lankveld, D.P., Bokkers, B.G., van Hoeven-Arentzen, P.H., Bouwmeester, H., Oomen, A.G., 2011. Presence and risks of nanosilica in food products. Nanotoxicology 5, 393–405.

Deniaud, A., Sharaf el dein, O., Maillier, E., Poncet, D., Kroemer, G., Lemaire, C., Brenner, C., 2008. Endoplasmic reticulum stress induces calcium-dependent permeability transition, mitochondrial outer membrane permeabilization and apoptosis. Oncogene 27, 285–299.

Dong, P., Li, J.H., Xu, S.P., Wu, X.J., Xiang, X., Yang, Q.Q., Jin, J.C., Liu, Y., Jiang, F.L., 2016. Mitochondrial dysfunction induced by ultra-small silver nanoclusters with a distinct toxic mechanism. J. Hazard. Mater. 308, 139–148.

Dorn 2nd, G.W., Vega, R.B., Kelly, D.P., 2015. Mitochondrial biogenesis and dynamics in the developing and diseased heart. Genes. Dev. 29, 1981–1991.

Du, Z., Zhao, D., Jing, L., Cui, G., Jin, M., Li, Y., Liu, X., Liu, Y., Du, H., Guo, C., Zhou, X., Sun, Z., 2013. Cardiovascular toxicity of different sizes amorphous silica nanoparticles in rats after intratracheal instillation. Cardiovasc. Toxicol. 13, 194–207.

Duan, J., Yu, Y., Li, Y., Huang, P., Zhou, X., Peng, S., Sun, Z., 2014a. Silica nanoparticles enhance autophagic activity, disturb endothelial cell homeostasis and impair angiogenesis. Part. Fibre Toxicol. 11, 50.

Duan, J., Yu, Y., Li, Y., Wang, J., Geng, W., Jiang, L., Li, Q., Zhou, X., Sun, Z., 2014b. Silica nanoparticles induce autophagy and endothelial dysfunction via the PI3K/Akt/mTOR signaling pathway. Int. J. Nanomed. 9, 5131–5141.

Duan, J.C., Yu, Y.B., Li, Y., Yu, Y., Li, Y.B., Zhou, X.Q., Huang, P.L., Sun, Z.W., 2013. Toxic effect of silica nanoparticles on endothelial cells through DNA damage response via Chk1-dependent G2/m checkpoint. PLoS One 8.

Duchen, M.R., 2000. Mitochondria and calcium: from cell signalling to cell death. J. Physiol. 529 (Pt 1), 57–68.

Fujioka, K., Hanada, S., Inoue, Y., Sato, K., Hirakuri, K., Shiraishi, K., Kanaya, F., Ikeda, K., Usui, R., Yamamoto, K., Kim, S.U., Manome, Y., 2014. Effects of silica and titanium oxide particles on a human neural stem cell line: morphology, mitochondrial activity, and gene expression of differentiation markers. Int. J. Mol. Sci. 15, 11742–11759.

Giedt, R.J., Pfeiffer, D.R., Matzavinos, A., Kao, C.Y., Alevriadou, B.R., 2012. Mitochondrial dynamics and motility inside living vascular endothelial cells: role of bioenergetics. Ann. Biomed. Eng. 40, 1903–1916.

Guerrero-Beltran, C.E., Bernal-Ramirez, J., Lozano, O., Oropeza-Almazan, Y., Castillo, E.C., Garza, J.R., Garcia, N., Vela, J., Garcia-Garcia, A., Ortega, E., Torre-Amione, G., Ornelas-Soto, N., Garcia-Rivas, G., 2017. Silica nanoparticles induce cardiotoxicity interfering with energetic status and Ca2+ handling in adult rat cardiomyocytes. Am. J. Physiol. Heart Circ. Physiol. 312, H645–H661.

Guo, C., Xia, Y., Niu, P., Jiang, L., Duan, J., Yu, Y., Zhou, X., Li, Y., Sun, Z., 2015. Silica nanoparticles induce oxidative stress, inflammation, and endothelial dysfunction in vitro via activation of the MAPK/Nrf2 pathway and nuclear factor-kappaB signaling. Int. J. Nanomed. 10, 1463–1477.

Guo, C., Yang, M., Jing, L., Wang, J., Yu, Y., Li, Y., Duan, J., Zhou, X., Sun, Z., 2016. Amorphous silica nanoparticles trigger vascular endothelial cell injury through apoptosis and autophagy via reactive oxygen species-mediated MAPK/Bcl-2 and PI3K/Akt/mTOR signaling. Int. J. Nanomed. 11, 5257–5276.

Guo, D., Bi, H., Wang, D., Wu, Q., 2013. Zinc oxide nanoparticles decrease the expression and activity of plasma membrane calcium ATPase, disrupt the intracellular calcium homeostasis in rat retinal ganglion cells. Int. J. Biochem. Cell. Biol. 45, 1849–1859.

Hackenberg, S., Scherzed, A., Kessler, M., Hummel, S., Technau, A., Froelich, K., Ginzkey, C., Koehler, C., Hagen, R., Kleinsasser, N., 2011. Silver nanoparticles: evaluation of DNA damage, toxicity and functional impairment in human mesenchymal stem cells. Toxicol. Lett. 201, 27–33.

He, C., Jiang, S., Jin, H., Chen, S., Lin, G., Yao, H., Wang, X., Mi, P., Ji, Z., Lin, Y., Lin, Z., Liu, G., 2016. Mitochondrial electron transport chain identified as a novel molecular target of SPIO nanoparticles mediated cancer-specific cytotoxicity. Biomaterials 83, 102–114.

Hill, B.G., Benavides, G.A., Lancaster Jr., J.R., Ballinger, S., Dell'Italia, L., Jianhua, Z., Darley-Usmar, V.M., 2012. Integration of cellular bioenergetics with mitochondrial quality control and autophagy. Biol. Chem. 393, 1485–1512.

Izyumov, D.S., Domnina, L.V., Nepryakhina, O.K., Avetisyan, A.V., Golyshev, S.A., Ivanova, O.Y., Korotetskaya, M.V., Lyamzaev, K.G., Pletjushkina, O.Y., Popova, E.N., Chernyak, B.V., 2010. Mitochondria as source of reactive oxygen species under oxidative stress. Study with novel mitochondria-targeted antioxidants–the "Skulachev-ion" derivatives. Biochemistry 75, 123–129.

Jaeger, A., Weiss, D.G., Jonas, L., Kriehuber, R., 2012. Oxidative stress-induced cytotoxic and genotoxic effects of nano-sized titanium dioxide particles in human HaCaT keratinocytes. Toxicology 296, 27–36.

Jendrach, M., Pohl, S., Voth, M., Kowald, A., Hammerstein, P., Bereiter-Hahn, J., 2005. Morpho-dynamic changes of mitochondria during ageing of human endothelial cells. Mech. Ageing Dev. 126, 813–821.

Ji, Z., Zhang, D., Li, L., Shen, X., Deng, X., Dong, L., Wu, M., Liu, Y., 2009. The hepatotoxicity of multi-walled carbon nanotubes in mice. Nanotechnology 20, 445101.

Kang, G.S., Gillespie, P.A., Gunnison, A., Moreira, A.L., Tchou-Wong, K.M., Chen, L.C., 2011. Long-term inhalation exposure to nickel nanoparticles exacerbated atherosclerosis in a susceptible mouse model. Environ. Health Perspect. 119, 176–181.

Keller, A.A., McFerran, S., Lazareva, A., Suh, S., 2013. Global life cycle releases of engineered nanomaterials. J. Nanoparticle Res. 15.

Lerner, C.A., Rutagarama, P., Ahmad, T., Sundar, I.K., Elder, A., Rahman, I., 2016. Electronic cigarette aerosols and copper nanoparticles induce mitochondrial stress and promote DNA fragmentation in lung fibroblasts. Biochem. Biophys. Res. Commun. 477, 620–625.

Li, J., Zhang, Y., Xiao, Q., Tian, F., Liu, X., Li, R., Zhao, G., Jiang, F., Liu, Y., 2011. Mitochondria as target of quantum dots toxicity. J. Hazard. Mater. 194, 440–444.

Liu, X., Sun, J.A., 2010. Endothelial cells dysfunction induced by silica nanoparticles through oxidative stress via JNK/P53 and NF-kappa B pathways. Biomaterials 31, 8198–8209.

Marzetti, E., Csiszar, A., Dutta, D., Balagopal, G., Calvani, R., Leeuwenburgh, C., 2013. Role of mitochondrial dysfunction and altered autophagy in cardiovascular aging and disease: from mechanisms to therapeutics. Am. J. Physiol. Heart Circ. Physiol. 305, H459–H476.

Maser, E., Schulz, M., Sauer, U.G., Wiemann, M., Ma-Hock, L., Wohlleben, W., Hartwig, A., Landsiedel, R., 2015. In vitro and in vivo genotoxicity investigations of differently sized amorphous SiO2 nanomaterials. Mutat. Res. Genet. Toxicol. Environ. Mutagen 794, 57–74.

Mills, N.L., Donaldson, K., Hadoke, P.W., Boon, N.A., MacNee, W., Cassee, F.R., Sandstrom, T., Blomberg, A., Newby, D.E., 2009. Adverse cardiovascular effects of air pollution. Nat. Clin. Pract. Cardiovasc. Med. 6, 36–44.

Nemmar, A., Albarwani, S., Beegam, S., Yuvaraju, P., Yasin, J., Attoub, S., Ali, B.H., 2014. Amorphous silica nanoparticles impair vascular homeostasis and induce systemic inflammation. Int. J. Nanomed. 9, 2779–2789.

Nguyen, K.C., Rippstein, P., Tayabali, A.F., Willmore, W.G., 2015. Mitochondrial toxicity of cadmium telluride quantum dot nanoparticles in mammalian hepatocytes. Toxicol. Sci. 146, 31–42.

Oberdorster, G., Maynard, A., Donaldson, K., Castranova, V., Fitzpatrick, J., Ausman, K., Carter, J., Karn, B., Kreyling, W., Lai, D., Olin, S., Monteiro-Riviere, N., Warheit, D., Yang, H., 2005. Principles for characterizing the potential human health effects from exposure to nanomaterials: elements of a screening strategy. Part. Fibre Toxicol. 2, 8.

Ong, S.B., Kalkhoran, S.B., Cabrera-Fuentes, H.A., Hausenloy, D.J., 2015. Mitochondrial fusion and fission proteins as novel therapeutic targets for treating cardiovascular disease. Eur. J. Pharmacol. 763, 104–114.

Orrenius, S., Gogvadze, V., Zhivotovsky, B., 2015. Calcium and mitochondria in the regulation of cell death. Biochem. Biophys. Res. Commun. 460, 72–81.

Puddu, P., Puddu, G.M., Galletti, L., Cravero, E., Muscari, A., 2005. Mitochondrial dysfunction as an initiating event in atherogenesis: a plausible hypothesis. Cardiology 103, 137–141.

Raoof, M., Mackeyev, Y., Cheney, M.A., Wilson, L.J., Curley, S.A., 2012. Internalization of C60 fullerenes into cancer cells with accumulation in the nucleus via the nuclear pore complex. Biomaterials 33, 2952–2960.
Raturi, A., Simmen, T., 2013. Where the endoplasmic reticulum and the mitochondrion tie the knot: the mitochondria-associated membrane (MAM). Biochim. Biophys. Acta 1833, 213–224.
Rejman, J., Nazarenus, M., Jimenez de Aberasturi, D., Said, A.H., Feliu, N., Parak, W.J., 2016. Some thoughts about the intracellular location of nanoparticles and the resulting consequences. J. Colloid Interface Sci. 482, 260–266.
Ren, J., Pulakat, L., Whaley-Connell, A., Sowers, J.R., 2010. Mitochondrial biogenesis in the metabolic syndrome and cardiovascular disease. J. Mol. Med. (Berlin, Ger.) 88, 993–1001.
Rocha, M., Apostolova, N., Hernandez-Mijares, A., Herance, R., Victor, V.M., 2010. Oxidative stress and endothelial dysfunction in cardiovascular disease: mitochondria-targeted therapeutics. Curr. Med. Chem. 17, 3827–3841.
Rodrigo, G.C., Standen, N.B., 2005. Role of mitochondrial re-energization and Ca2+ influx in reperfusion injury of metabolically inhibited cardiac myocytes. Cardiovasc. Res. 67, 291–300.
Scaini, G., Fries, G.R., Valvassori, S.S., Zeni, C.P., Zunta-Soares, G., Berk, M., Soares, J.C., Quevedo, J., 2017. Perturbations in the apoptotic pathway and mitochondrial network dynamics in peripheral blood mononuclear cells from bipolar disorder patients. Transl. Psychiatry 7, e1111.
Shenouda, S.M., Widlansky, M.E., Chen, K., Xu, G., Holbrook, M., Tabit, C.E., Hamburg, N.M., Frame, A.A., Caiano, T.L., Kluge, M.A., Duess, M.A., Levit, A., Kim, B., Hartman, M.L., Joseph, L., Shirihai, O.S., Vita, J.A., 2011. Altered mitochondrial dynamics contributes to endothelial dysfunction in diabetes mellitus. Circulation 124, 444–453.
Souza, N.H., Ferrari, R.A., Silva, D.F., Nunes, F.D., Bussadori, S.K., Fernandes, K.P., 2014. Effect of low-level laser therapy on the modulation of the mitochondrial activity of macrophages. Braz J. Phys. Ther. 18, 308–314.
Sun, L., Li, Y., Liu, X., Jin, M., Zhang, L., Du, Z., Guo, C., Huang, P., Sun, Z., 2011. Cytotoxicity and mitochondrial damage caused by silica nanoparticles. Toxicol. In Vitro 25, 1619–1629.
Szabadkai, G., Duchen, M.R., 2008. Mitochondria: the hub of cellular Ca2+ signaling. Physiol. (Bethesda) 23, 84–94.
Tvrda, E., Kovacik, A., Tusimova, E., Paal, D., Mackovich, A., Alimov, J., Lukac, N., 2016. Antioxidant efficiency of lycopene on oxidative stress - induced damage in bovine spermatozoa. J. Anim. Sci. Biotechnol. 7, 50.
Wang, L.M., Liu, Y., Li, W., Jiang, X.M., Ji, Y.L., Wu, X.C., Xu, L.G., Qiu, Y., Zhao, K., Wei, T.T., Li, Y.F., Zhao, Y.L., Chen, C.Y., 2011. Selective targeting of gold nanorods at the mitochondria of cancer cells: implications for cancer therapy. Nano Lett. 11, 772–780.
Wang, W., Li, Y., Liu, X., Jin, M., Du, H., Liu, Y., Huang, P., Zhou, X., Yuan, L., Sun, Z., 2013. Multinucleation and cell dysfunction induced by amorphous silica nanoparticles in an L-02 human hepatic cell line. Int. J. Nanomed. 8, 3533–3541.
Wenz, T., 2009. PGC-1alpha activation as a therapeutic approach in mitochondrial disease. IUBMB Life 61, 1051–1062.
Wilson, C.L., Natarajan, V., Hayward, S.L., Khalimonchuk, O., Kidambi, S., 2015. Mitochondrial dysfunction and loss of glutamate uptake in primary astrocytes exposed to titanium dioxide nanoparticles. Nanoscale 7, 18477–18488.
Xia, T., Kovochich, M., Brant, J., Hotze, M., Sempf, J., Oberley, T., Sioutas, C., Yeh, J.I., Wiesner, M.R., Nel, A.E., 2006. Comparison of the abilities of ambient and manufactured nanoparticles to induce cellular toxicity according to an oxidative stress paradigm. Nano Lett. 6, 1794–1807.
Xu, Y., Wang, N., Yu, Y., Li, Y., Li, Y.B., Yu, Y.B., Zhou, X.Q., Sun, Z.W., 2014. Exposure to silica nanoparticles causes reversible damage of the spermatogenic process in mice. PLoS One 9, e101572.
Xue, Y., Chen, Q., Ding, T., Sun, J., 2014. SiO(2) nanoparticle-induced impairment of mitochondrial energy metabolism in hepatocytes directly and through a Kupffer cell-mediated pathway in vitro. Int. J. Nanomed. 9, 2891–2903.
Youle, R.J., van der Bliek, A.M., 2012. Mitochondrial fission, fusion, and stress. Science 337, 1062–1065.
Yu, E., Mercer, J., Bennett, M., 2012. Mitochondria in vascular disease. Cardiovasc. Res. 95, 173–182.
Yu, X., Hong, F., Zhang, Y.Q., 2016. Bio-effect of nanoparticles in the cardiovascular system. J. Biomed. Mater. Res. Part A 104, 2881–2897.
Zhang, D.X., Gutterman, D.D., 2007. Mitochondrial reactive oxygen species-mediated signaling in endothelial cells. Am. J. Physiol. Heart Circ. Physiol. 292, H2023–H2031.
Zhu, M.T., Wang, B., Wang, Y., Yuan, L., Wang, H.J., Wang, M., Ouyang, H., Chai, Z.F., Feng, W.Y., Zhao, Y.L., 2011. Endothelial dysfunction and inflammation induced by iron oxide nanoparticle exposure: risk factors for early atherosclerosis. Toxicol. Lett. 203, 162–171.
Zhu, Y., Zhao, Q., Li, Y., Cai, X., Li, W., 2006. The interaction and toxicity of multi-walled carbon nanotubes with Stylonychia mytilus. J. Nanosci. Nanotechnol. 6, 1357–1364.
Zuo, L., Li, Q., Sun, B., Xu, Z., Ge, Z., 2013. Cilostazol promotes mitochondrial biogenesis in human umbilical vein endothelial cells through activating the expression of PGC-1alpha. Biochem. Biophys. Res. Commun. 433, 52–57.